Int. J. Electrochem. Sci., 12 **(2017)** 1130 – 1145, doi: 10.20964/2017.02.16

International Journal of
ELECTROCHEMICAL
SCIENCE
www.electrochemsci.org

Electrodeposition and Behavior of Palladium in a Room-temperature Ionic Liquid

Xiaoli Xi[*], *Shanshan Song, Zuoren Nie, Liwen Ma*

College of Material Science and Engineering, Beijing University of Technology, Beijing 100124, China
[*]E-mail: xixiaoli@bjut.edu.cn

Received: 9 October 2016 / *Accepted:* 30 November 2016 / *Published:* 30 December 2016

This paper reports the electrodeposition of Pd in the room-temperature ionic liquid 1-ethyl-3-methylimidazolium trifluoroacetate ([emim]TA). The electrochemical behavior of $PdCl_2$ in [emim]TA was investigated using cyclic voltammetry. Cyclic voltammograms were recorded at various scan rates and temperatures and showed that the reduction of Pd was irreversible. The diffusion coefficient of $PdCl_2$ in [emim]TA increased with increasing temperature and the diffusion activation energy was determined to be 43.66 KJ mol^{-1}. The optimum parameters of Pd electrodeposition in [emim]TA were determined through single-factor experiments. The surface morphology of the deposits was analyzed via scanning electron microscopy and the crystal structure of metallic Pd was confirmed through X-ray diffraction.

Keywords: Palladium; [emim]TA; Electrochemical behavior; Electrodeposition

1. INTRODUCTION

Given its excellent physical and chemical properties, the noble metal palladium (Pd) has various applications including use in electrical devices and catalysis. [1]. However, China has scarce reserves of precious metals and Pd resources have significantly decreased due to the exploitation of raw ores [2]. With the development of the electronic industry and the increase of consumption in electronic-related products in China, both the demand for Pd and the amount of electronic waste containing significant quantities of Pd have also increased. For example, outdated printed circuit boards contain large amounts of precious metals, including 0.01 wt% of Pd [3]. Due to the rapid replacement of modern mobile phones, the amount of electronic waste has increased. Thus, it is of great importance to develop a method for the recovery of Pd from secondary resources, especially electronic waste.

As a method of metal recovery, hydrometallurgy displays remarkable advantages over pyrometallurgy including higher metal recovery, lower initial monetary investment and energy consumption, and smaller operation scale. Hydrometallurgical processes for Pd recovery include chemical precipitation [4,5], adsorption [6], ion exchange [7–9], and solvent extraction [10–12]. Compared to the present technologies, electrochemistry provides an effective way to recover metals and offers the advantages of lower equipment cost, convenient operation conditions, and direct access to the products at the end of the process. Electrodeposition properties such as surface morphology [13] and particle size can be controlled and nanoscale metals can be prepared [14] by tuning electrochemical parameters such as potential, current density, electrolyte composition, and temperature. Common electrolysis systems include aqueous solutions and high-temperature molten salts. The latter requires an electrolytic medium with a high melting point, which can be a complicated procedure. Therefore, electrodeposition in aqueous solutions can be slightly more convenient. Yang [15] analyzed the electrodeposition and electrocrystallization behavior of Pd on a glass/carbon electrode and proved that additives inhibit Pd electrodeposition and reduce hydrogen release. Some studies also investigated the electrodeposition behavior of Pd on Pt and stainless steel electrodes in a nitric acid medium [16,17] and showed that the Faraday current efficiency decreases by increasing the concentration of nitric acid. The decrease in Faraday current efficiency is due to the co-reduction of nitric acid and H^+ ions. Palladium is an active element of the Pt-group metals that demonstrates high catalytic activity, low overpotential, and strong H_2 absorbability. Statistics show that spongy or powdered Pd may absorb 900 times its volume in H_2, resulting in high internal stresses within the coating, which decreases production quality and current efficiency [1,18]. Thus, the primary limitation of electrolysis in aqueous solutions is related to hydrogen evolution. Additives can improve deposit quality, but they can also make the electrolyte composition more complicated. In recent years, room-temperature ionic liquids have been widely applied in many fields due to their special advantages, such as insignificant vapor pressure, high stability, wide electrochemical window, and solubility for both multiple organic and inorganic compounds. The ionic structure and wide electrochemical window of room-temperature ionic liquids make them ideal electrolytic media for the direct electrodeposition of metals from organic solutions at ambient temperature [19,20], especially nanocrystalline materials that are difficult to electrodeposit in aqueous solutions or organic phases [14]. The melting point of ionic liquids is lower than 373 K and the nonaqueous nature of ionic liquids causes only negligible amounts of hydrogen to be released during electrodeposition. Thus, the operational conditions and product quality are more convenient and superior than traditional electrolysis systems.

Recent studies have used extraction as the electrodeposition process [21,22] to recover Pd from nitric acid and fast reactor-simulated high-level liquid waste. In this novel method, TOMAC was used as the ionic liquid, which exists in the semi-solid state at 298 K and benzene and $CHCl_3$ were added as additives. However, $CHCl_3$ has a high vapor pressure, which substantially decreases the volume of the organic phase. To improve this process, Kumaresan [23] replaced $CHCl_3$ with DIPB, by using TBP as a modifier, and adopted the same process to recover Pd. Although the possibility of electrodepositing Pd directly in the organic phase was proven, a low current efficiency of ~30% was achieved. With the development of ionic liquids, quaternary phosphonium ionic liquids have attracted attention for such processes, due to their capacity to weaken the electrostatic interaction between cations and anions, their relatively low viscosity and their high conductivity [24–26]. However, there is currently insufficient information regarding quaternary phosphonium ionic liquids. Previous studies analyzed the electrochemical behavior of two Pd-halide complexes, $[PdBr_4]^{2-}$ and $[PdCl_4]^{2-}$ in pyrrolidinium ionic liquids (BMPTFSI) at 298 K [1,27]. It was found that this anion-containing ionic liquid ($TFSI^-$) is advantageous due to its hydrophobicity; albeit, it is more expensive compared to other ionic liquids. The imidazolium ionic liquid, bmimCl has also been reported for its applications in the electrodeposition of Pt-group metals [28–30]. Researchers mainly analyzed the electrochemical behavior of signal metals and their ternary or binary solutions in bmimCl, and observed the surface morphology of the electrodeposits. However, due to the high melting point of bmimCl (341 K), the electrodeposition required a higher temperature (373 K) to ensure appropriate conditions. We have previously studied 1-ethyl-3-methylimidazolium trifluoro-methanesulfonate, ([emim]OTf) as an ionic liquid with relatively low melting point and viscosity through single-factor experiments and we have obtained the optimum parameters for Pd electrodeposition [31]. Additionally, we have discovered 1-ethyl-3-methylimidazolium trifluoroacetate, ([emim]TA) as a novel electrolysis medium for Pd that has the potential to demonstrate superior properties compared to [emim]OTf. Therefore, the present study aims to investigate the Pd electrolysis medium [emim]TA.

2. EXPERIMENTAL

2.1 Materials

All of the chemicals used in this research were analytical grade. 1-Ethy-3-methylimidazolium trifluoroacetate ([emim]TA) containing a purity higher than 99% was procured by Shanghai Cheng jie Chemical Co. Ltd., China. Palladium(II) chloride containing a purity higher than 99% was procured from Sinopharm Chemical Reagent Co., Ltd., Beijing, China.

2.2 Electrochemical behavior and electrodeposition of Pd in [emim]TA

A $PdCl_2$ solution in [emim]TA (approximately 12 mM) was prepared in order to investigate the electrochemical behavior of $PdCl_2$ through cyclic voltammetry. In addition, the mole ratio for electrodeposition mentioned in this paper indicates the ratio of the amount of substance between [emim]TA and $PdCl_2$. In detail we experimented with a mole ratio of 50~70 to determine the optimum value. A homemade, three-electrode cell was used. Platinum wires (Φ 0.5 mm) were used as both working and counter electrodes, while Pd wire (Φ1 mm) was used as the reference electrode. Another experiment, galvanostatic electrodeposition, was performed on a Ti plate (15×5) by employing DC power equipment (Agilent Technologies E361×A). The Ti plates were used as both substrate and counter electrodes, and the Pd wire was used as the reference electrode. The substrate was used as the cathode and the counter electrode was connected to a Pd wire which was used as the anode. Following electrodeposition, it was observed that the deposits had either attached onto the substrate or fallen into the electrolyte, with the latter being collected through centrifugation. Both of the deposits were thoroughly rinsed with alcohol, dilute hydrochloric acid, and deionized water, and then dried in order to examine surface morphology and phase analysis. The above operations were performed within an Ar-filled glove box.

2.3 Instrumentation

The cyclic voltammograms of the various solutions were measured using an electrochemical workstation (model ZAHNER IM6e). The surface morphology of the deposits was examined by a SU-8020 field emission scanning electron microscope and the elemental composition was determined using an energy-dispersive spectrometer at a voltage of 15.0 KV. The phase analysis of the deposits was characterized via X-ray diffraction (XRD-7000).

3. RESULTS AND DISCUSSION

3.1 Electrodeposition of Pd in [emim]TA

Figs. 1(a) and 1(b) show the electrochemical window of [emim]TA and the cyclic voltammogram of Pd (II) chloride in [emim]TA that is recorded at 298 K. The inset is a larger version of Fig. 1(b).

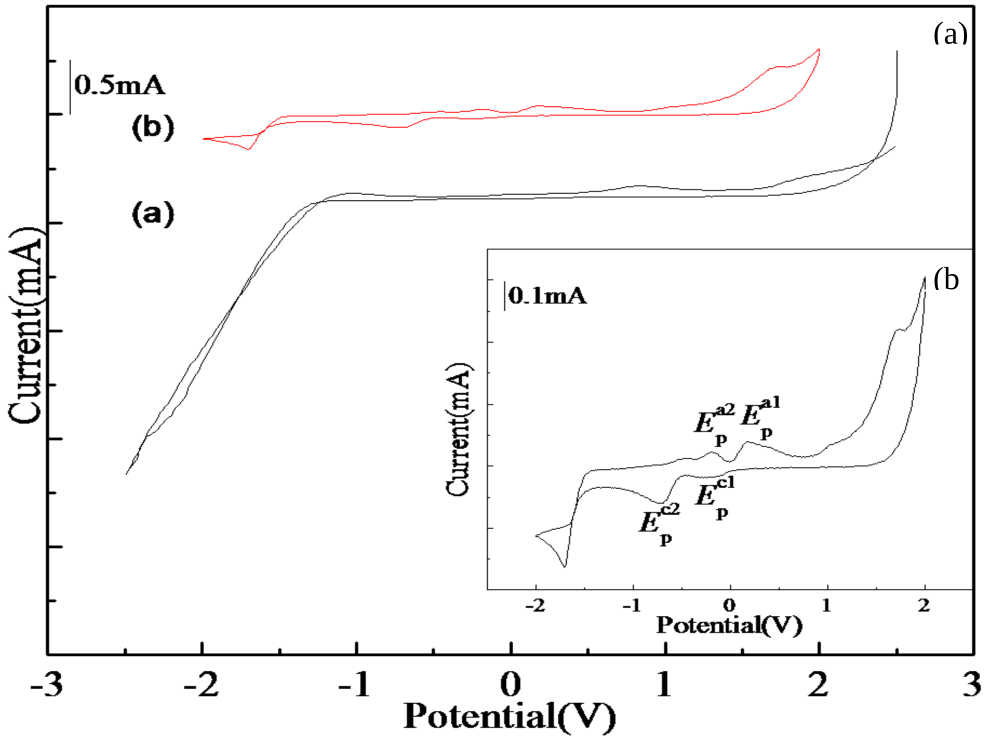

Figure 1. Electrochemical window of [emim]TA (a) and cyclic voltammograms of Pd (II) chloride in [emim]TA (b). T=298K; Scan rate: 50mV/s; Working and counter electrodes: Pt wire; Reference electrode: Pd wire; Mole ratio of [emim]OTf and $PdCl_2$: 45:1.

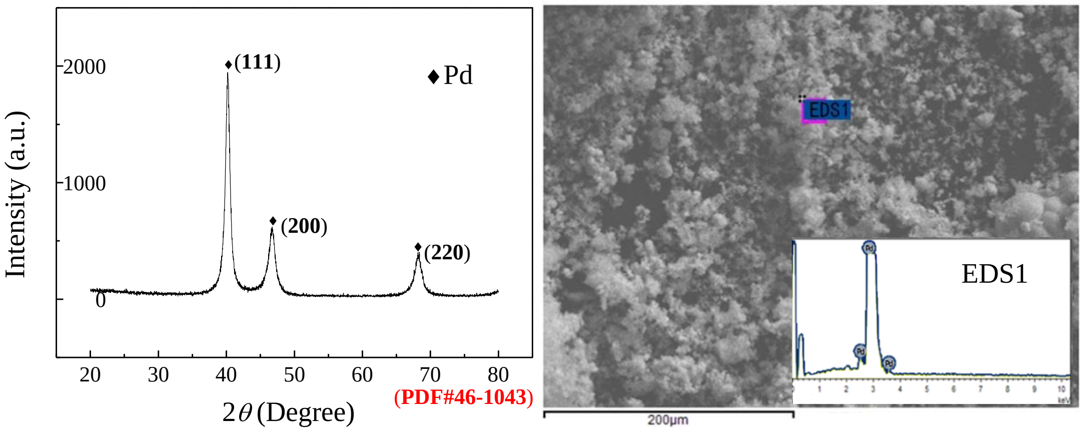

(a) (b)

Figure 2. XRD pattern (a) and EDS pattern (b) of the electrodeposits from [emim]TA, performed by galvanostatic electrodeposition.

In our operation condition, the ionic liquid 1-ethyl-3-methylimidazolium trifluoromethanesulfonate exhibited an electrochemical window at almost 3.0V (vs. Pd), which was wider than the reported ionic liquid bmimCl (2.5V at 373K) [19]. When scanning in the negative The mole ratio between [emim]TA and $PdCl_2$ was 45 and the scan rate was 50 mV s^{-1}. The electrochemical window of the [emim]TA was approximately 2.95 V (from −1.26 V to 1.69 V) at room temperature. When scanning in the negative direction, both weak and prominent reduction waves were observed at approximately −0.3 and −0.7 V, respectively. On the contrary, when scanning in the reverse direction, two oxidation waves were observed. The current density was determined using the reduction peak current at −0.7 V and the surface area of the working electrode that was immersed into the electrolyte. Additionally, galvanostatic electrodeposition was carried out at 298 K employing an electrolysis time of 22 h and an electrode distance of 23 mm. After electrodeposition, part of the deposits was attached to the substrate while the remaining of the deposits fell into the electrolytic cell via centrifugation until the collection was complete. The above phenomenon was similar to that described in reference [13]. The deposits were analyzed via XRD and EDS, the results of which are presented in Fig. 2. The deposits consisted of high-purity metallic Pd, indicating that the ionic liquid [emim]TA may act as an ideal electrolytic medium for Pd-electrodeposition.

3.2 Electrochemical behavior of Pd(II) in [emim]TA

The electrochemical windows of [emim]TA for the temperature range of 303–323 K are presented in Fig. 3 (a). Fig. 3 indicates that the electrochemical window of [emim]TA remained constant at approximately 3.0 V, within the experimental error. When $PdCl_2$ was added, the scan range was set from −1.2 V to 1.5 V, and the temperature range was set from 303 K to 323 K. The analysis process for the kinetics of Pd(II) in [emim]TA at the above temperatures was similar, and the process at 313 K was used for the following discussion.

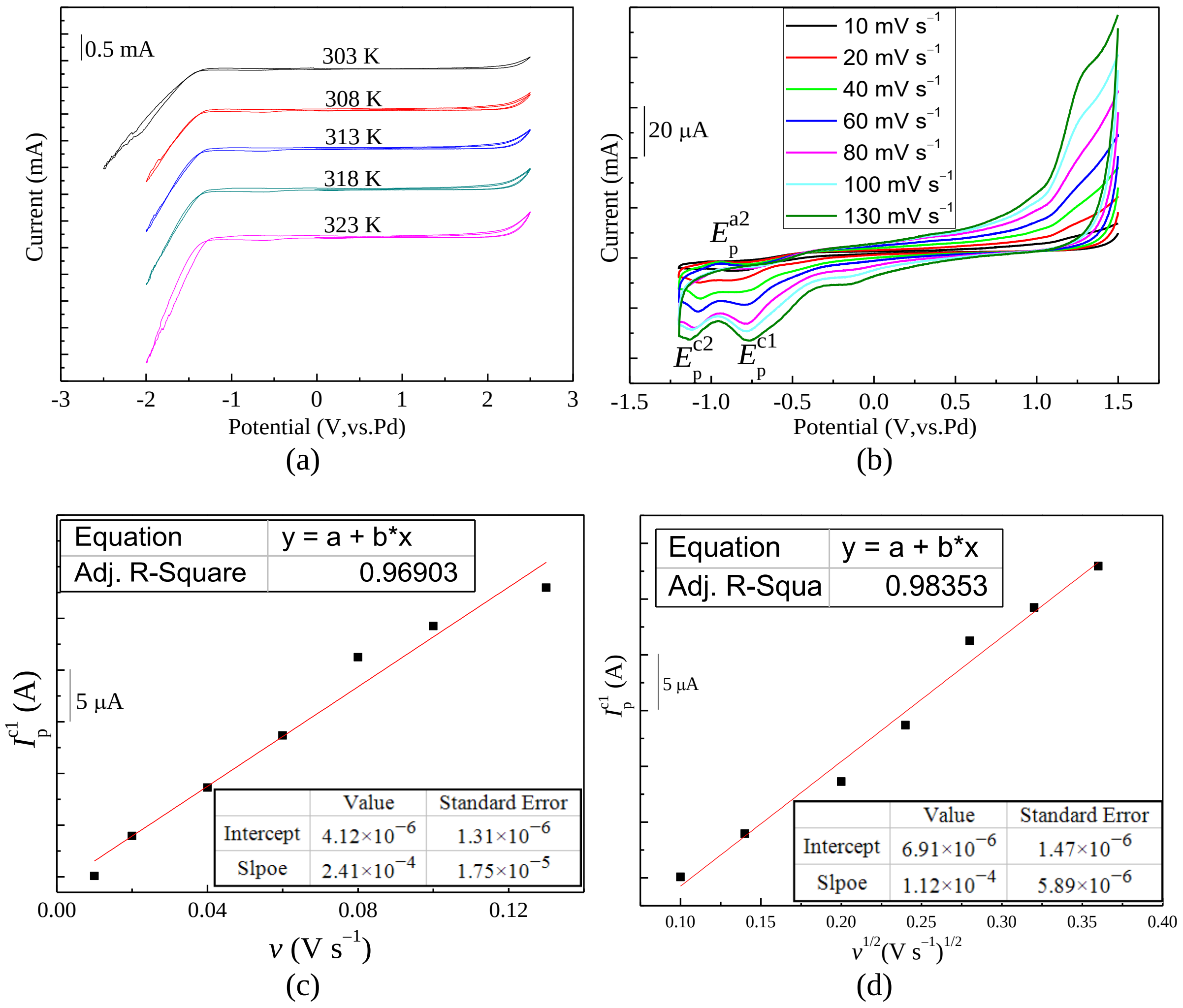

Figure 3. Electrochemical window of (a) [emim]TA from 303K – 323 K, cyclic voltammograms and (b) [emim]TA-PdCl$_2$ for 10–130 mV s^{-1} at 313 K; relationship between reduction peak current I_p^{c1} and v (c) or $v^{1/2}$ (d) at 313 K. Scan rate: 50mV/s; Working and counter electrodes: Pt wire; Reference electrode: Pd wire; Mole ratio of [emim]OTf and PdCl$_2$: 45:1.

The cyclic voltammograms of PdCl$_2$ in [emim]TA (12 mM) for scan rates between 10–130 mV s^{-1} are presented in Fig. 3 (b). Two prominent reduction waves (E_p^{c1} and E_p^{c2}) were observed from −0.75 V to −1.2 V when scanning in the negative direction; increasing the scan rate increased the reduction peak current. In addition, the reduction peak currents in the positive potential were significantly higher than the reduction peak currents in the negative potential. This indicates that the reduction rate below the value of E_p^{c1} is higher than that below E_p^{c2} [32]. When scanning in the reverse direction, a weak oxidation wave E_p^{a2} appeared from −1.0 V to −0.9 V, which corresponds to the reduction wave E_p^{c2}. The amplitude of E_p^{a2} became gradually wider by increasing the scan rate. The oxidation wave E_p^{a2} disappeared at scan rates over 100 mV s^{-1} and the oxidation waves that corresponded to E_p^{c1} were not observed when scanning was performed in the positive direction. These data suggest that the oxidation peak currents were significantly lower than the corresponding reduction waves. Moreover, the difference in ($E_p^{a} - E_p^{c}$) was approximately 139 mV (at a rate of 60 mV s^{-1}), considerably higher than the difference recorded during the reversible process ($E_p^{a} - E_p^{c} \approx 2.3\ RT/(nF) \approx 31$ mV, at 313 K). This indicates that the reduction on the Pt working electrode is irreversible. The data of E_p^{c1} obtained at scan rates between 10–130 mV s^{-1} are presented in **Error! Reference source not found.**.

Table 1. Data of cyclic voltammograms with sweeping rates between 10–130 mV s^{-1} at 313 K.

v (mV s^{-1})	$v^{1/2}$ $(V\ s^{-1})^{1/2}$	E_p^{c1} (V vs.Pd)	I_p^{c1} (mA)	$E_{p/2}$ (V vs.Pd)	$\mid E_p-E_{p/2} \mid$ (V vs.Pd)	αn_α
10	0.1	−0.867	−0.00509	−0.662	0.205	0.24
20	0.14	−0.896	−0.00896	−0.664	0.232	0.22
40	0.2	−0.844	−0.01363	−0.586	0.258	0.19
60	0.24	−0.793	−0.01868	−0.565	0.228	0.22
80	0.28	−0.781	−0.02624	−0.544	0.237	0.21
100	0.32	−0.781	−0.02925	−0.502	0.279	0.18
130	0.36	−0.769	−0.03296	−0.457	0.312	0.16
Average						0.20

The charge transfer coefficient α for an irreversible electrode process can be expressed as follows [32]:

$$\mid E_p - E_{p/2} \mid = 1.857\ RT/(\alpha n_\alpha F) \qquad \text{Eq. (3-1)}$$

where $E_{p/2}$ is the half-peak potential, n_α is the number of electrons in the control step, F is the Faraday constant, and T is the absolute temperature in K. The average value of αn_α was 0.20 at 313 K. Furthermore, the plot of the reduction peak current I_p^{c1} as a function of the scan rate v and the square root of scan rate ($v^{1/2}$) are presented in Fig. 3 (c) and (d), respectively. The comparison between the R-square and the standard error of the fitting lines showed that the plot of I_p^{c1} as a function of $v^{1/2}$ conformed to a linear relationship. This confirms that the electrodeposition of Pd in [emim]TA was determined by diffusion mechanisms. The relation between I_p^{c1} and $v^{1/2}$ for an irreversible process can be expressed as follows [28,29]:

$$I_p^c = 0.4958 nFC_0^* AD^{1/2}((\alpha n_\alpha)Fv/(RT))^{1/2} \qquad \text{Eq. (3-2)}$$

where C_0^* is the concentration of Pd(II) in mol cm^{-3}, A is the electrode area in cm^2, n is the number of exchanged electrons, D is the diffusion coefficient in $cm^2\ s^{-1}$, and v is the scan rate in V s^{-1}. By considering the value of αn_α and the slope of the straight line in Fig. 3 (d), the value of the diffusion coefficient D_1 at 313 K was estimated at 5.58×10^{-7} $cm^2\ s^{-1}$. The D-values for the remaining temperatures were between (3.07-9.60) $\times 10^{-7}$ $cm^2\ s^{-1}$. This indicates that increasing the temperature gradually increased the diffusion coefficients of Pd(II) in [emim]TA as a consequence of both the gradual decrease in ionic liquid viscosity. Increasing the temperature of the electrolyte caused a decrease in the diffusion resistance of the electroactive substances in the electrolyte.

Comparing to our previous report [31], the diffusion coefficients calculated in the two studies were different at the same temperature. There are two possibilities to account for the different D-values. As the only difference between two electrolysis system is the type of anion from the ionic liquid, different Pd species can form via complexation with the various anions. Another possibility is the existence of Pd as a Pd-chloro complex; however, the resistance from ions of the ionic liquid is different. It should be noted that if Pd was complexed with Cl^- when dissolved in the ionic liquid, then the reduction potential in our two reports would be similar due to the same operation conditions; however, the reduction potential was significantly different [31]. In addition, if Pd was complexed with Cl^-, three types of Pd species would be observed due to the formation of three different Pd-chloro complexes [33, 34]; however, only two reduction waves were observed in the presented CV curves. Based on the analysis above, Cl^- would be replaced by CF_3COO^- (TA^-) when dissolving $PdCl_2$ into [emim]TA. Consequently, it can be concluded that the type of the anion in ionic liquid can influence the kinetic behavior of electroactive substance, the type of Pd(II) species dissolved in ionic liquids, and the reaction mechanism [35].

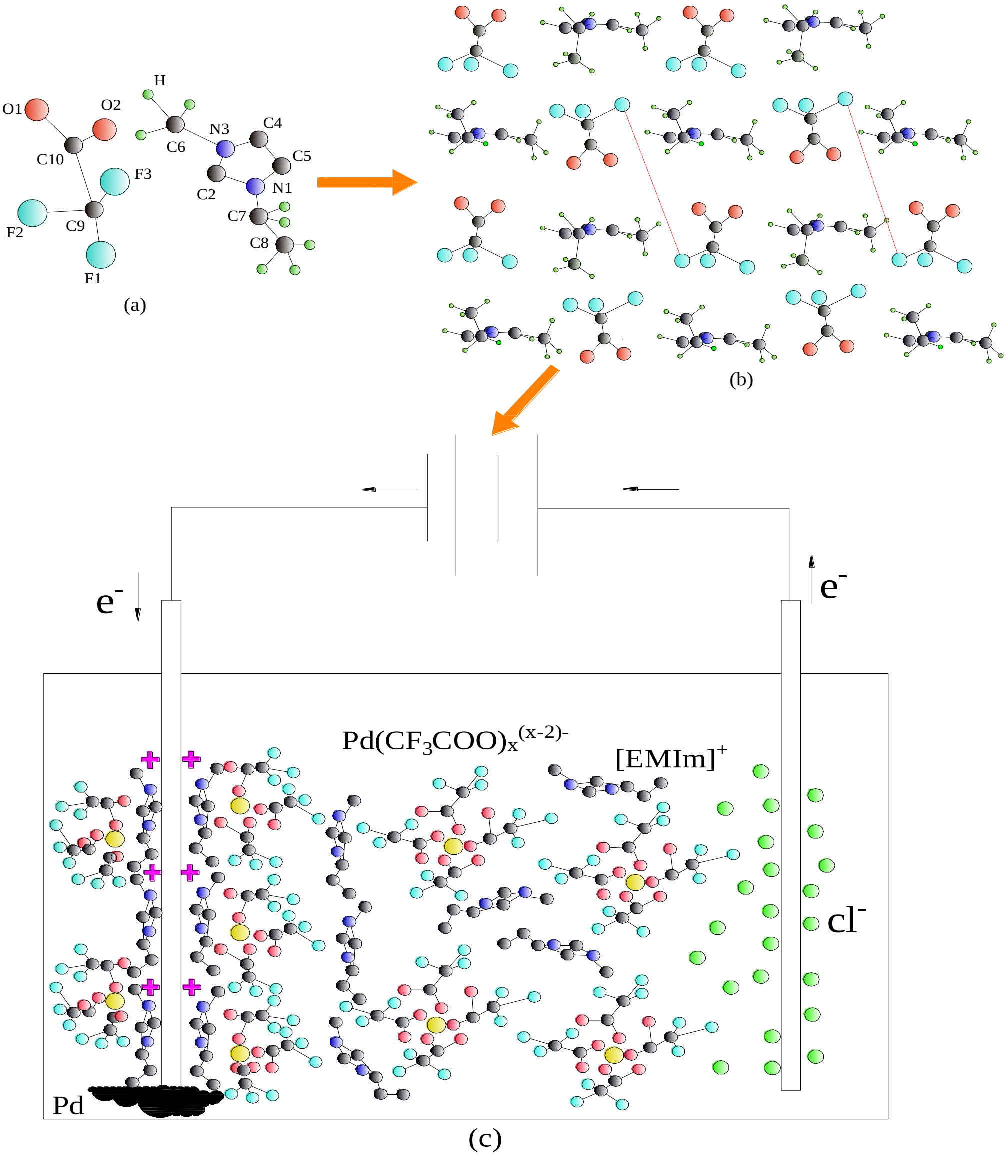

Figure 4. Molecular models of [emim]TA (a), (b) and reaction process of electrodeposition Pd in [emim]TA (c).

In addition, two reduction waves were observed in the electrochemical window of [emim]TA. It was postulated that both waves were due to the reduction of Pd(II) to Pd(0). As the stability of Pd complexes in [emim]TA is different, the order of reduction changes based on the complex stability. This behavior has been reported in *N*-butyl-*N*-methylpyrrolidinium dicyanamide ionic liquid (BMP-DCA) [36] and in 1-butyl-3-methylimidazolium chloride ionic liquid (BMICl) [28]. The Pd species existed in [emim]TA was proposed to be $[Pd(CF_3COO)_x]^{(x-2)-}$, and the reaction during reduction occurred via a single step and as a two-electron process as follows:

$$[Pd(CF_3COO)_x]^{(x-2)-} + 2e^- \rightarrow Pd(0)+x(CF_3COO)^- \qquad \text{Eq. (3-3)}$$

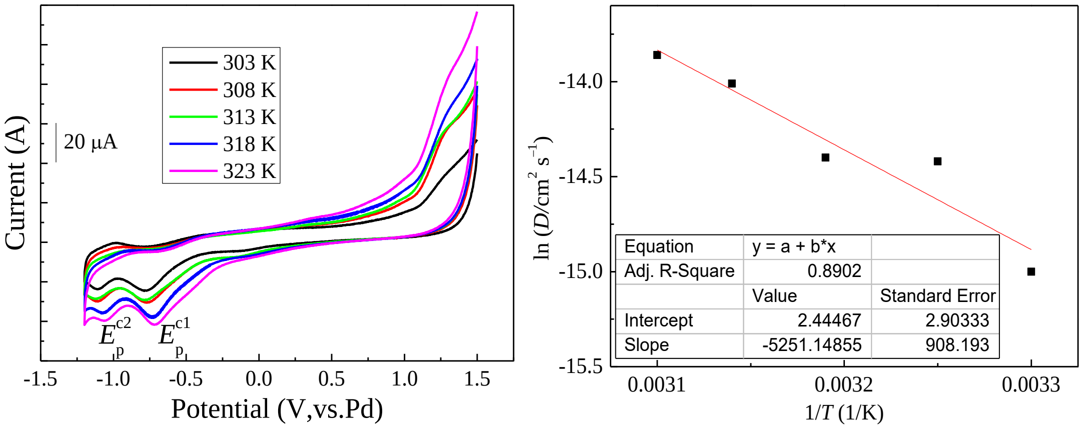

Equation	y = a + b*x	
Adj. R-Square	0.8902	
	Value	Standard Error
Intercept	2.44467	2.90333
Slope	-5251.14855	908.193

(a) (b)

Figure 5. Cyclic voltammograms of (a) $[emim]TA\text{-}PdCl_2$ at 303K -323K; Relationship between ln*D* and 1/*T* and (b) $[emim]TA\text{-}PdCl_2$; Scan rate: 100mV/s; Working and counter electrodes: Pt wire; Reference electrode: Pd wire; Mole ratio of [emim]OTf and $PdCl_2$: 45:1.

The reaction process for the electrodeposition of Pd in [emim]TA is shown in Fig. 4. According to the ORTEP-III of [emim]OTf given in [37], the single molecular model and packing diagram of [emim]TA are shown in Fig. 4 (a) and (b), respectively. The imidazolium rings are arranged in an ABAB…order, the $–CF_3$ group of the anion points towards the cationic imidazolium ring, and the anions of the adjacent are connected to each other via F…F interactions [37]. Based on the conclusion above, when $PdCl_2$ was added into [emim]TA, Pd(II) complexes were formed with TA^-. Due to the effect of electric field stress, a layer of $[emim]^+$ will be electrostatically attracted on the working electrode surface, forming an electrode/electrolyte interface. The ordering into layers decreases further from the substrate. After the innermost of $[emim]^+$ layer, alternating layers of anions and cations would be expected, as shown in Fig.4 (c). This phenomenon has been verified via a combination of AFM, STM and CV experiments [38,34]. During the process of electrodeposition, black deposits can be observed around the cathode, which have been identified as metallic Pd. Considering the conservation of electric charge, it can be inferred that Cl^- would be released during electrolysis and from discharging at the anode under the electric field force.

The effect of temperature on cyclic voltammograms is demonstrated in Fig. 5 (a). As the temperature increased, the reduction peak current gradually increased and the potential of the reduction waves shifted towards the positive direction. This confirms that an increase in temperature accelerates the diffusion rate of ions and decreases both the polarization efficiency and the overpotential of reduction, causing the reduction potential to shift towards positive values.

The increase in the diffusion coefficients of Pd(II) by increasing the temperature indicates that both parameters conform to the Arrhenius equation [28]:

$D=Ae^{(-E_a/(RT))}$ Eq. (3-4)

where A is the pre-exponential factor and E_a is the activation energy. The relation between ln$D$ and $1/T$ is demonstrated in Fig. 5 (b). The activation energy for Pd(II) ions was calculated at 43.66 KJ mol^{-1} using the slope of the trend line. Single-factor experiments were conducted to acquire the optimum parameters of Pd electrodeposition in [emim]TA and the results are discussed as follows.

3.3 Temperature

Temperature affects the viscosity and the conductivity of ionic liquids, the thermal movement and the diffusion rate of Pd ions and the energy for nucleation and growth. This study investigated the effect of temperature on the electrodeposition of Pd(II) in [emim]TA by analyzing both the cathodic current efficiency and the recovery of metallic Pd. The initial temperature was 298 K and was controlled by a thermostatic oil bath. The current density was 0.016 mA mm^{-2}, the mole ratio between the [emim]TA and the $PdCl_2$ was 60, the electrode distance was 23 mm, and the electrolysis duration was 10 h. The current efficiency was calculated as follows:

$\eta= m'/(cIt) \times 100$, Eq. (3-5)

where η is the current efficiency, $m'$is the actual amount of deposits (g), I is the current (A), t is the electrolysis duration (h), and c is the electrochemical equivalent (g A^{-1} h^{-1}). The effect of temperature on current efficiency and recovery is demonstrated in Fig.6 (a). Initially, the current efficiency was significantly increased by increasing the temperature, then slowly increased until 313 K. At this point, a maximum value for current efficiency was achieved, followed by a decrease in current efficiency as the temperature continued to increase. The recovery of Pd was calculated as follows:

$$\eta_{\text{Recovery}}=\frac{m_{\text{Recovery}}}{m_{\text{PdCl}_2}\times\frac{M_{\text{Pd}}}{M_{\text{PdCl}_2}}}\times 100 \qquad \text{Eq. (3-6)}$$

where m_{Recovery} is the actual amount of deposits (g), m_{PdCl2} is the mass of $PdCl_2$ added into [emim]TA, and M_{Pd} and M_{PdCl2} are the relative molecular masses of Pd (106.42) and $PdCl_2$ (177.31), respectively. When the original mass of Pd in the solution was consistent, Pd recovery was proportional to the mass of deposits. The calculated results showed a similar trend to the current efficiency; that is, current efficiency initially increased to a maximum value (59.44 %) at 308 K, then reached a plateau while the temperature continued to increase before finally decreasing at 318 K. When the temperature was further increased to 323 K, the cathode substrate cracked following the electrodeposition; thus, heating was terminated. The viscosity of the ionic liquid decreased with increasing temperature and promoted the diffusion rate of ions, which further increased the amount of Pd(II) ions discharged onto the cathode. Thus, both the current efficiency and the Pd recovery increased. However, if the temperature continued to increase, then anti-dissolution would occur. This phenomenon may cause some deposits to re-dissolve into the electrolyte at high temperatures; therefore, decreasing the amount of collected deposits. On the basis of the analysis above, the optimum temperature was selected as 308 K.

3.4 Current density

The current density values applied for Pd electrodeposition in [emim]TA ranged from 0.012 mA mm^{-2} to 0.034 mA mm^{-2}. The temperature was set at 308 K, the mole ratio between [emim]TA and $PdCl_2$ was 60, the electrolysis duration was 10 h, and the electrode distance was 23 mm. The cathode current efficiency and recovery of the metallic Pd were calculated by using Equations (3-5) and (3-6), and the results are presented in Fig. 6 (b).

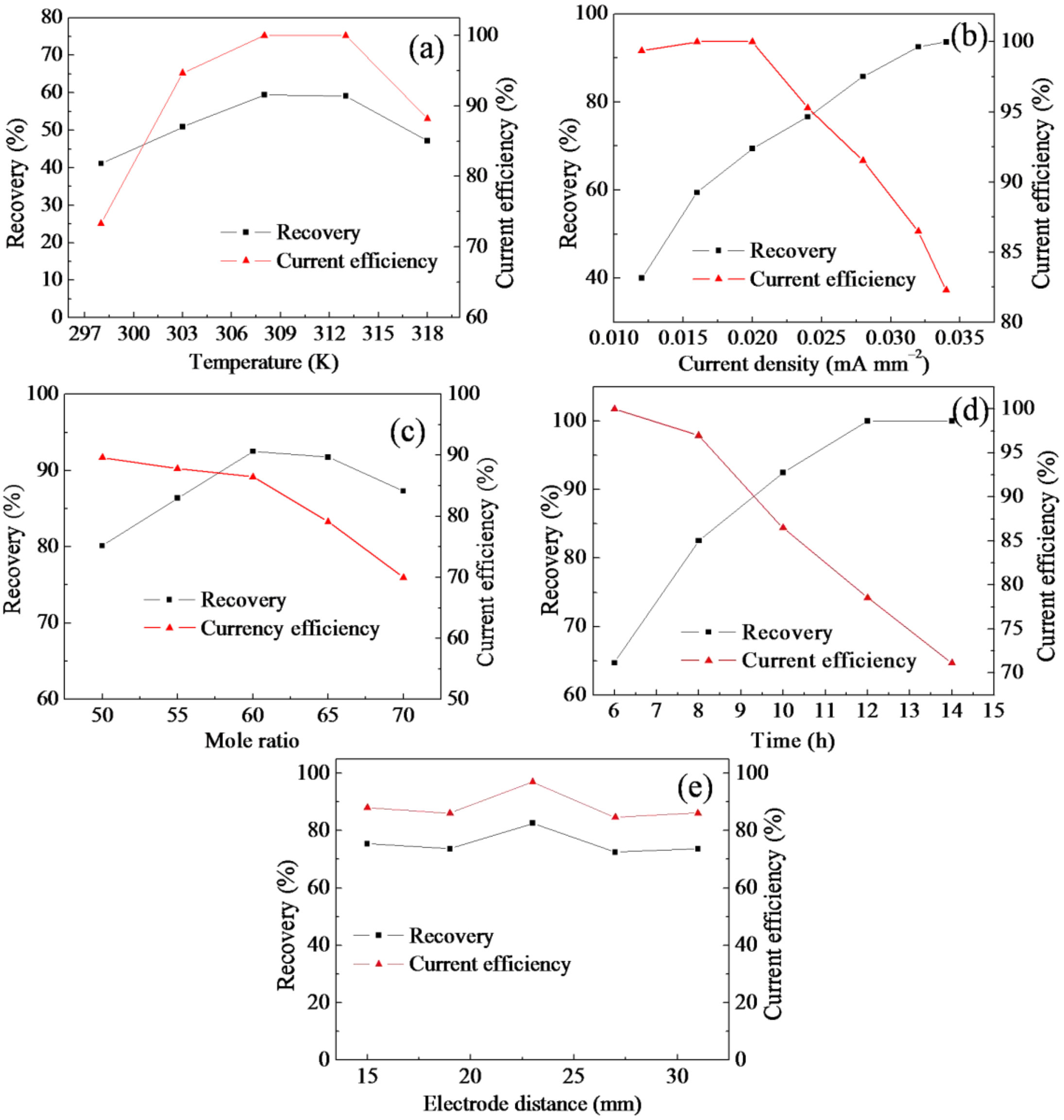

Figure 6. Effect of temperature (a), current density (b), mole ratio (c), electrolysis time (d), and electrode distance (e) on the current efficiency and recovery of electrodeposited Pd. (Parameters that were kept constant are as follows: temperature 308 K, current density 0.016 mA mm^{-2}, mole ratio 60, electrolysis time 10 h, electrode distance 23 mm.)

When the current density increased from 0.012 mA mm^{-2} to 0.020 mA mm^{-2}, the current efficiency slightly increased. This observation could be attributed to experimental error. However, the current efficiency appeared to decrease as polarization increased. The recovery continuously increased during the entire process, which conforms to Faraday's Law. This result indicates that the mass of the deposits is directly proportional to the quantity of the electrical charges that pass through the electrolyte. The comparison of the two curves, when the current density ranged from 0.012 mA mm^{-2} to 0.032 mA mm^{-2}, showed that the increase in recovery was always higher than the decrease in current efficiency. When deposition was performed at 0.032 mA mm^{-2}, the current efficiency was 86.48 % and the recovery was 92.5 %. When the current density was 0.034 mA mm^{-2}, the recovery still slightly increased by 1.1 %, and the current efficiency decreased by 4.2 %. On the basis of the analysis above, 0.032 mA mm^{-2} was selected as the optimum current density.

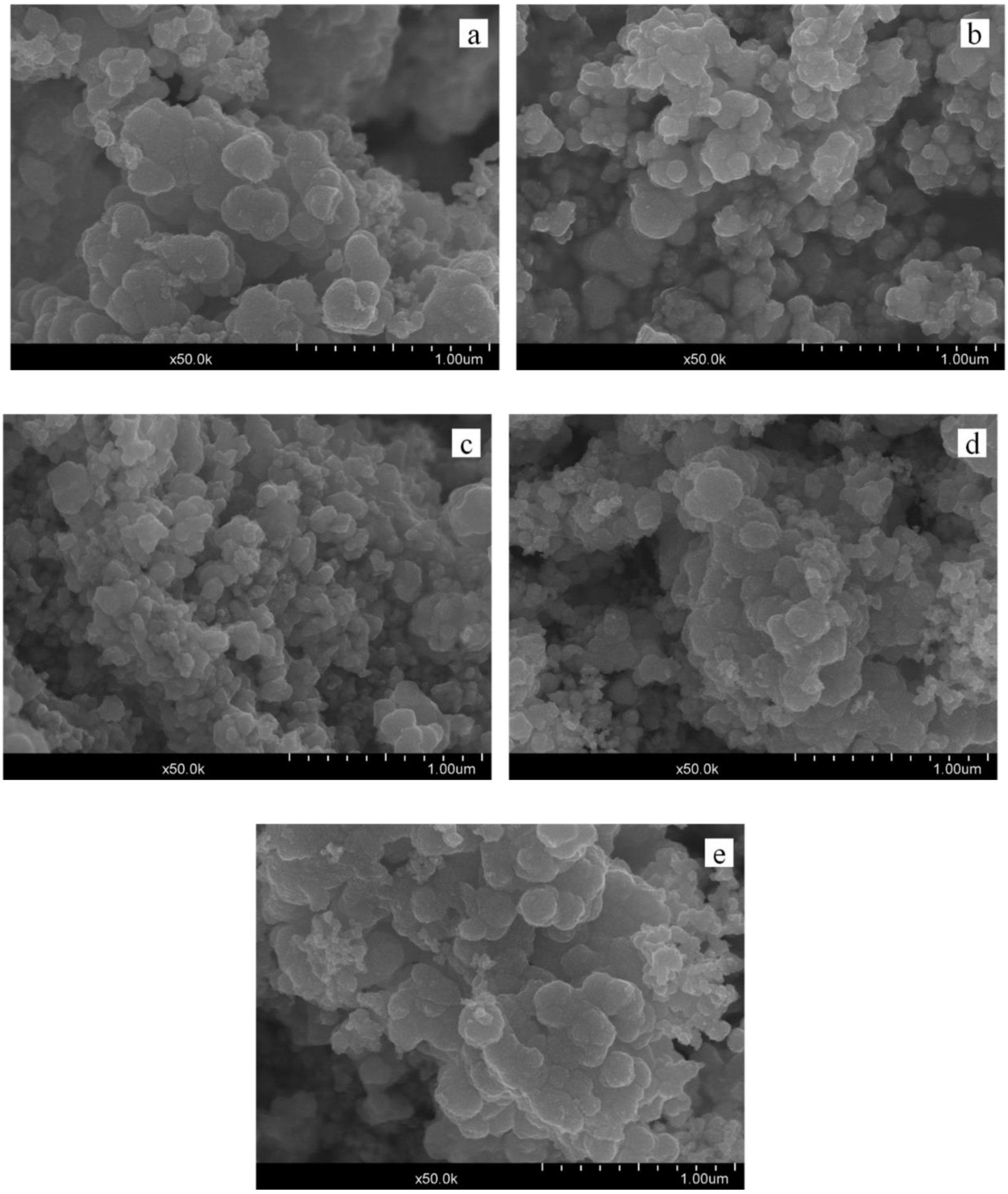

Figure 7. SEM morphology of Pd electrodeposited in [emim]TA at different applied current densities of 0.012 (a), 0.016 (b), 0.024 (c), 0.028 (d), and 0.032 mA mm^{-2} (e). (Parameters that were

kept constant are as follows: temperature 308 K, mole ratio 60, electrolysis time 10 h, electrode distance 23 mm.)

The surface morphology of the deposits at different current densities was also analyzed, and the results are presented in Fig. 7.

When compared at the same magnification, the scanning electron micrographs showed that the deposits obtained from [emim]TA-$PdCl_2$ were primarily spherical, and that the average particle size initially decreased and then increased with increasing current density. The increase in current density enhanced cathodic polarization, improved the nucleation rate, and gradually decreased the average particle size. However, when the current density reached 0.028 mA mm^{-2}, the redundant energy of the products obtained resulted in the growth of the crystal nucleus. Therefore, the average particle size gradually increased due to the increase in the system energy.

3.5 Mole ratio of [emim]TA and $PdCl_2$

The mole ratio of [emim]TA and $PdCl_2$ ranged from 50 to 70, the temperature was 308 K, the current density was 0.032 mA mm^{-2}, the electrolysis duration was 14 h, and the electrode distance was 23 mm. The effect of mole ratio on current efficiency and recovery is demonstrated in Fig. 6 (c).

When the mole ratio of [emim]TA and $PdCl_2$ ranged from 50 to 70, the proportion of Pd(II) in the electrolyte decreased, consequently, the current efficiency also decreased. In detail, the current efficiency slightly decreased, when the mole ratio ranged from 50 to 60, and then substantially decreased, when the mole ratio was greater than 60. Additionally, the recovery reached a maximum value of 92.5 %, when the mole ratio was 60, and then decreased when the mole ratio continued to increase. On the basis of the above analysis, the amount of Pd(II) ions in the solution gradually decreased by increasing the mole ratio of [emim]TA and $PdCl_{2.}$ which consequently weakened the ion collisions and enhanced the diffusion rate of Pd(II) ions. However, electrolysis decreased the concentration of Pd(II) and the concentration gradient in the electrolyte may have induced concentration polarization. The current efficiency was primarily affected by concentration polarization, which was enhanced when the mole ratio was higher than 60. According to equation (3-6), the calculation for recovery is related to the mass ratio of deposits and $PdCl_2$ added into the electrolyte. As presented in Fig. 6 (c), when the mole ratio was lower than 60, the current efficiency slightly decreased, suggesting that both the amount of electrodeposits slightly changed. Additionally, when the mole ratio was higher than 60, the amount of electrodeposits significantly decreased. Moreover, the amount of $PdCl_2$ added into the solution constantly decreased. Thus, the calculated recovery initially increased and then slightly decreased. In summary, the optimum mole ratio was determined to be 60.

3.6 Electrolysis duration

The electrolysis duration was set from 6 h to 14 h, the electrolysis temperature was 308 K, the current density was 0.032 mA mm^{-2}, the mole ratio of [emim]TA and $PdCl_2$ was 60, and the electrode distance was 23 mm. The influence of electrolysis duration on current efficiency and recovery is demonstrated in Fig. 6 (d).

The current efficiency slowly decreased from 6 h to 8 h and the value was 96.95 % at 8 h. When the electrolysis duration was prolonged (from 8h to 14h), the decrease in the amplitude of current efficiency (25.81 %) was higher than the increase in recovery of Pd (17.47%). Following 14 h of electrolysis, the current efficiency was decreased to 71.14 %. The recovery of Pd constantly increased, particularly from 6 h to 8 h, during which the increase ranged from 64.69 % to 82.53 %. The increase in amplitude of recovery decreased with prolonged electrolysis time. When the electrode reaction was completed with prolonged electrolysis time, the recovery of Pd gradually increased. However, excessive electrolysis duration can cause concentration polarization and trigger the loss of electric charges in the connection of each part of the circuit, which can have a significant impact on current efficiency [39]. Considering the both aspects, 8 h was selected as the optimum electrolysis time.

3.7 Electrode distance

The electrode distance was set at 15, 19, 23, 27, or 31 mm; the electrolysis temperature was 308 K, the current efficiency was 0.032 mA mm^{-2}, the mole ratio of [emim]TA and $PdCl_2$ was 60, and the electrolysis duration was 8 h (Fig. 6(e)).

The overall space volume of electrolytic cell was limited. Under the conditions described above, the effect of the electrode distance on both the current efficiency and the recovery of Pd was minimal and the slight fluctuation of values at different parameters can be as attributed to experimental error.

In conclusion, the maximum current efficiency of electrodeposited Pd on [emim]TA was 96.95%, and the recovery of Pd was 82.53% under the optimum conditions. Both the current efficiency and the recovery of Pd were higher in [emim]TA compared to ionic liquid [emim]OTf [31].

4. CONCLUSIONS

1. Pd was electrodeposited in a new ionic liquid electrolytic medium, 1-ethy-3-methylimidazolium trifluoroacetate ([emim]TA), at room temperature.
2. Two prominent reduction waves were observed. The first reduction wave was observed when scanning in the negative direction which can be attributed to the reduction of Pd(II) to Pd(0) and one weak oxidation wave appeared when scanning in the opposite direction.
3. The electrochemical window of [emim]TA was about 3.0 V and the electrode process for the electrodeposition of Pd in [emim]TA was controlled by diffusion mechanisms. The diffusion coefficient was ~10^{-7} cm^2 s^{-1} from 303–323 K and the activation energy for the diffusion of Pd(II) in [emim]TA was 43.66 KJ mol^{-1}.
4. The current efficiency and the recovery of electrodeposited Pd in [emim]TA were 96.59 % and 82.53 %, respectively, under the optimum parameters.

ACKNOWLEDGEMENTS
This research was financially supported by the National Natural Science Foundation of China (No. 51422401 and No. 51304010).

References

1. Y. Bando, Y. Katayama, T. Miura, *Electrochim Acta,* 53 (2007) 87-91.
2. G.Q. Fu, X.X. Fan, H.G. Dong, *Precious Met,* 34 (2013) 75-79.
3. Y. Chehade, A. Siddique, H. Alayan, *International Conference on Chemical, Civil and Environment engineering,* (2012) 226-231.
4. S. Sarioglan, *Platin Met Rev,* 57 (2013) 289-296.
5. M.A. Barakat, G.A. EL-Mahdy, M. Hegazy, *The Open Mineral Processing Journal,* 2 (2009) 31-36.
6. Y. Xiong, C.R. Adhikari, H. Kawakita, K. Ohto, K. Inoue, H. Harada, *Bioresource Technol,* 100 (2009) 4083-4089.
7. L. Labosova, M. Stofkova, J. Kracunovska, *Acta Metall Slov,* 12 (2006) 235-241.
8. E. Schoeman, S.M. Bradshaw, G. Akdogan, *The Southern African Institute of Mining and Metallurgy Platinum,* (2012) 729-740.
9. A.N. Nikoloski, K.L. Ang, *Min Proc Ext Met Rev,* 35 (2014) 369-389.
10. C.Y. Peng, T.H. Tsai, *Desalin Water Treat,* 47 (2012) 105-111.
11. B.R. Reddy, B. Raju, J.Y. Lee, H.K. Park, *J Hazard Mater,* 180 (2010) 253-258.
12. N. Papaiconomou, J.M. Lee, J. Salminen, M. von Stosch, J.M. Prausnitz, *Ind Eng Chem Res,* 47 (2008) 5080-5086.
13. M. Jayakumar, K.A. Venkatesan, R. Sudha, T.G. Srinivasan, P.R.V. Rao, *Mater Chem Phys,* 128 (2011) 141-150.
14. F. Endres, M. Bukowski, R. Hempelmann, H. Natter, *Angew Chem Int Edit,* 42 (2003) 3428-3430.
15. F.Z. Yang, L. Huang, S.K. Xu, S.M. Zhou, *Acta Phys-Chim Sin,* 20 (2004) 463-467.
16. M. Jayakumar, K.A. Venkatesan, T.G. Srinivasan, P.R.V. Rao, *Electrochim Acta,* 54 (2009) 1083-1088.
17. S.C. Liu, R.Q. Liu, Y. Wu, Y.Z. Wei, B.Z. Fang, *3rd International Conference on Asian Nuclear Prospects (Anup2012),* 39 (2013) 387-395.
18. J.M. Yu, *Market Analysis,* 1 (2007) 46-47.
19. P.R.V. Rao, K.A. Venkatesan, T.G. Srinivasan, *Prog Nucl Energ,* 50 (2008) 449-455.
20. K.A. Venkatesan, C.H. JagadeeswaraRao, K. Nagarajan, *Int J Electrochem,* (2012) 1-8.
21. M. Jayakumar, K.A. Venkatesan, T.G. Srinivasan, P.R.V. Rao, *J Appl Electrochem,* 39 (2009) 1955-1962.
22. P. Giridhar, K.A. Venkatesan, T.G. Srinivasan, P.R.V. Rao, *Hydrometallurgy,* 81 (2006) 30-39.
23. R. Kumaresan, R. Jain, K.A. Venkatesan, M.P. Antony, B.M. Bhanage, *J Radioanal Nucl Ch,* 303 (2015) 1047-1052.
24. Q. Huang, L.L. Wang, B.Z. Zheng, Q. Long, *Prog Chem,* 21 (2009) 1782-1791.
25. M. Matsumiya, S. Suda, K. Tsunashima, M. Sugiya, S. Kishioka, H. Matsuura, *J Electroanal Chem,* 622 (2008) 129-135.
26. K. Tsunashima, M. Sugiya, *Electrochem Commun,* 9 (2007) 2353-2358.
27. Y. Katayama, Y. Bando, T. Miura, *T I Met Finish,* 86 (2008) 205-210.
28. M. Jayakumar, K.A. Venkatesan, T.G. Srinivasan, *Electrochim Acta,* 52 (2007) 7121-7127.
29. M. Jayakumar, K.A. Venkatesan, T.G. Srinivasan, *Electrochim Acta,* 53 (2008) 2794-2801.
30. M. Jayakumar, K.A. Venkatesan, T.G. Srinivasan, P.R.V. Rao, *Electrochim Acta,* 54 (2009) 6747-6755.
31. X.L. Xi, S.S. Song, Z.R. Nie, L.W. Ma, *Int J Electrochem Sc,* 10 (2015) 9179-9191.

32. Z. Jia, C.S. Da, L. Chen, *Chemical industry press, Beijing, PP,* (2006) 134-142.
33. S. Shrestha, E. Gjoka, E.J. Biddinger, *Molten Salts and Ionic Liquids 19,* 64 (2014) 267-274.
34. S. Shrestha, E.J. Biddinger, *Electrochim Acta,* 174 (2015) 254-263.
35. M. Xu, D.G. Ivey, Z. Xie, W. Qu, *Electrochim Acta,* 89 (2013) 756-762.
36. H.Y. Huang, P.Y. Chen, *Electrochim Acta,* 56 (2011) 2336-2343.
37. A.R. Choudhury, N. Winterton, A. Steiner, A.I. Cooper, K.A. Johnson, *Crystengcomm,* 8 (2006) 742-745.
38. R. Atkin, S.Z. El Abedin, R. Hayes, L.H.S. Gasparotto, N. Borisenko, F. Endres, *J Phys Chem C,* 113 (2009) 13266-13272.
39. H. Zhao, L.B. Xu, J.F. Chen, P.Y. Zhang, *Chin J Nonferrous Met,* 22 (2012) 2688.